

# Optimization of biodiesel production from Allamanda Seed Oil using design of experiment

Khadijat Abdullahi<sup>a,b</sup>, Sunday Samuel Ojonugwa<sup>a</sup>, Adeyinka Sikiru Yusuff<sup>c</sup>, Musa Umaru<sup>a</sup>, Ibrahim Aris Mohammed<sup>a</sup>, Moses Aderemi Olutoye<sup>a</sup>, Folorunsho Aberuagba<sup>a,\*</sup>

<sup>a</sup> Department of Chemical Engineering, Federal University of Technology Minna, Niger State, Nigeria

<sup>b</sup> Scientific Equipment Development Institute, Tagwai Dam Road, Minna, Niger State, Nigeria

<sup>c</sup> Department of Chemical Engineering, College of Engineering, Afe Babalola University, Ado-Ekiti, Nigeria

## ARTICLE INFO

### Keywords:

Allamanda oil  
Biodiesel  
Catalyst  
Metakaolin  
Transesterification

## ABSTRACT

KOH-modified metakaolin (KMK) was synthesized, characterized and utilized as a heterogeneous catalyst for biodiesel production from allamanda seed oil (ASO) for the first time. The effect of variables (temperature, time and catalyst concentration) affecting biodiesel production process was optimized using Box-Behnken design of response surface methodology. The biodiesel produced was consequently characterized to determine its fuel properties. Optimization results showed that maximum biodiesel yield of  $90.67 \pm 0.14\%$  was achieved at fixed methanol/ASO molar ratio of 5:1 and at the optimum conditions of  $52.5^\circ\text{C}$  reaction temperature, 180 min reaction time and 0.5 wt.% catalyst concentration. The properties of the produced biodiesel were comparable to the ASTM D6751 and EN 14214 specifications, thus indicating the suitability of the ASO biodiesel as a possible alternative to petroleum diesel.

## 1. Introduction

Biodiesel is a clean renewable fuel that can serve as a possible alternative to petroleum diesel. It is often derived from vegetable oil and animal fat through transesterification process [1–3]. Biodiesel is characterized by higher flash point, higher lubricity, higher combustion efficiency, higher cetane number, biodegradability, renewability, non-toxicity, and longer durability in diesel engines and environmentally friendliness due to its lower carbon monoxide emissions compared to conventional fossil fuels [4].

In almost all commercial processes for biodiesel production, edible oils are used as feedstock. Commercial production of biodiesel from edible oil in the developing economy like Nigeria is not very feasible since the nation cannot satisfy the food requirements of these oils [5]. Furthermore, the high prices of these oils can also increase the overall cost of biodiesel production [6–8]. One way of reducing the biodiesel production cost is to use cheaply available non-edible oils, animal fats, waste cooking oil and algae [9–12,13]. Allamanda (golden trumpet) flowers bear seed that contains approximately 57 wt% oil, indicating that it could serve as an attractive bio-oil bearing feedstock for biodiesel synthesis [14]. Another approach will be to avoid the use of

homogenous catalysts whose applications are limited to refined vegetable oils with free fatty acids (FFA) values of less than 0.5 wt-% [15]. The inherent insensitivity of heterogeneous catalysts to the presence of FFA, its lower toxicity, the recoverability and reusability, reduced corrosion tendency and ease of separation from the reaction product stream have made solid catalysts relatively promising catalysts for the synthesis of biodiesel from triglyceride-containing feedstock [16,17].

Kaolin is an aluminosilicate material which contains silica ( $\text{SiO}_2$ ), alumina ( $\text{Al}_2\text{O}_3$ ), iron oxide ( $\text{Fe}_2\text{O}_3$ ), titania ( $\text{TiO}_2$ ) and traces of other metal oxides. The large octahedral aluminium content makes kaolin resistant to acids. This type of clay material can be used as a heterogeneous catalyst in transesterification reactions [18]. Raw kaolin clay has almost no acidic or basic sites, and to improve its activity, it is essential to modify its framework with acid or alkali, leading to formation of metakaolin which possesses characteristics similar to zeolite LTA [19]. The use of kaolin-based catalyst in transesterification and esterification of vegetable oils and FFA with alcohols has rapidly increased [20]. Dang et al. [19] transesterified soybean with methanol to produce biodiesel over NaOH-modified kaolin catalyst at  $90^\circ\text{C}$  for 24 h which resulted in biodiesel yield of 97%. A tungstophosphoric acid impregnated kaolin was used as a catalyst for the esterification of oleic acid, resulting in

\* Corresponding author at: Department of Chemical Engineering, Federal University of Technology, Minna, Niger State, Nigeria.

E-mail addresses: [yusuffas@abuad.edu.ng](mailto:yusuffas@abuad.edu.ng) (A.S. Yusuff), [f.aberuagba@futminna.edu.ng](mailto:f.aberuagba@futminna.edu.ng) (F. Aberuagba).

**Table 1**  
Experimental design for biodiesel production process.

Variables	-1	0	+1
Time (min) A	60	120	180
Temperature (°C) B	40	52.5	65
Catalyst concentration (%wt.) C	0.5	2.75	5.0

97.21% conversion [21]. Furthermore, the synthesis of biodiesel via the transesterification of used cooking oil over methoxide-modified kaolin has been reported. The highest triglyceride conversion of 99.48% was achieved, indicating better performance of the catalyst in methanolysis process [18].

However, several works showed that varying one variable at a time (OVAT) method was used to evaluate the impact of process variables. This method is time-consuming and requires an unreliable number of experiments. In addition to these, OVAT technique is not capable to optimize and achieve true optimal conditions in a multivariant system such as biodiesel production process. One of the experimental design techniques that are commonly used for process analysis and modeling is response surface methodology (RSM). RSM is an efficient statistical process optimization design for determining an optimal condition in a multivariable system. It involves a set of mathematical and statistical methods for modelling and process analysis [22]. This methodology is suitable for optimizing systems whose response is influenced by numerous parameters [23–25]. With the use of RSM, estimation of linear, interaction and quadratic effects of the process variables and prediction model for the process output (response) are possible. The experimental data required are dependent on the selected design: central composite or Box-Behnken designs [12]. These are different in the number of runs required and in the combinations of the levels used in the experiment. The Box-Behnken design (BBD) is thought to be more capable and powerful than the central composite design (CCD) because it requires fewer experiments and has been shown to be adequate in describing the majority of steady-state process responses [12].

However, studies on the alkaline treatment of typical Nigerian kaolin (Kutigi Kaolin) and characterization as a catalyst for biodiesel production using RSM to provide an explicit understanding of the effect of process variables on biodiesel yield have not been documented to the best of the authors' knowledge. Thus, the present work aimed to investigate the potential of alkaline functionalized metakaolin as a heterogeneous catalyst for biodiesel production from allamanda seed oil. Box-Behnken design was applied to study the influence of process variables (temperature, reaction time and catalyst concentration) on biodiesel yield. Biodiesel produced was characterized to determine its physicochemical and fuel properties.

## 2. Materials and methods

### 2.1. Materials and chemicals used

Allamanda seeds were sourced from Ciromawa Estate, Bosso Road, Minna, Nigeria. The entire chemicals used in this study, including methanol (CH<sub>3</sub>OH, 95%), n-hexane (95%, Analar BDH) carbon tetrachloride (CCl<sub>4</sub>, 96%), potassium hydroxide pellet (KOH, 95%, Burgoyne & Co, India), Wij's solution, potassium iodide solution (KI, 92% M & B England), sodium thiosulphate (95%, M & B England), Phenolphthalein, and hydrochloric acid, are of analytical grade.

### 2.2. Oil extraction from Allamanda seeds

The endocarp and mesocarp layers of the collected seeds were removed to obtain the nuts. Thereafter, the obtained nuts were pulverized using mortar and pestle, dried and ground using a mechanical grinder. To extract oil from the *Allamanda* seeds powder, 15 g of the powder was placed in the thimble and was inserted into the chamber of

the Soxhlet extractor. 250 mL of n-hexane was poured into the round bottom flask and the Soxhlet was heated to 60–65 °C and was operated for 6 h. The extracted oil was poured into a beaker and heated on a hot plate at 105 °C to remove the residual solvent. The oil yield (Y) was then calculated using Eq. (1):

$$Y = \frac{\text{weight of oil}}{\text{weight of allamanda seed powder used on dry matter basis}} \times 100\% \quad (1)$$

Thereafter, the extracted *Allamanda* seed oil (ASO) was characterized to gain insights into its physicochemical properties (moisture content, specific gravity, acid value, viscosity, free fatty acid (FFA), saponification value, peroxide value and iodine value) which would reveal its suitability for biodiesel production.

### 2.3. Preparation and characterization of KOH-modified metakaolin (KMM) catalyst

The raw kaolin was first beneficiated, dried in an oven for 48 h at 170 °C and then sieved to obtain a particle size of 250 μm. The finely powdered kaolin was thereafter calcined in a furnace at 650 °C for 90 min to obtain metakaolin which was later activated by adding 20 g of it to KOH solution and stirred on a magnetic stirrer at 90 °C for 3 h. The resultant slurry was then allowed to cool and then washed with deionized water until pH of the washed water was almost neutral. The washed sample was dried in an oven at 100 °C overnight. The obtained KOH-modified metakaolin will henceforth be referred to as KMM.

The textural characteristics of the prepared KMM catalyst were evaluated using Quantachrome instrument (Autosorb-1 model No. 11.03, Florida, USA) at 77 K using liquid nitrogen. Surface morphology of the as-synthesized KMM catalyst was determined by scanning electron microscope (SEM, JEOL-JSM 5600 LV) equipped with a energy dispersive X-ray spectrometer (6587 EDS detector), while the phases and crystallographic structures of the catalyst were identified using Bragg–Brentano powder X-ray diffractometer with CuKα radiation (λ = 1.54184 Å). The elemental oxide compositions of the KMM catalyst were analysed by XRF spectroscopy (XRF—Oxford, ED-2000, England).

### 2.4. Catalytic activity during transesterification of ASO

The reactions were carried out in a 500 cm<sup>3</sup> glass reactor placed on a magnetic stirrer at atmospheric pressure. The fixed 50 ml of ASO and the desired amount of the metakaolin activated with KOH catalysts (0.5–5.0 wt%) were charged into the reactor, and then the methanol was introduced to the oil at constant methanol to oil ratio of 5:1. The reaction was operated at 40–65 °C with a varied reaction time of 60–180 min. After the reaction was completed, the reaction mixture was allowed to stand for 5 min before it was poured into a separating funnel to separate the biodiesel phase from the glycerol phase. The biodiesel was repeatedly washed with warm water until the wash water becomes colourless. The biodiesel was dried on a hot plate at 105 °C to remove residual water and the yield was calculated using Eq. (2).

$$\text{Yield} = \frac{\text{mass of biodiesel}}{\text{mass of oil}} \times 100 \quad (2)$$

#### 2.4.1. Characterization of produced ASO biodiesel

The physicochemical properties of the produced ASO biodiesel, such as kinematic viscosity, density, specific gravity, flash point, cloud point, pour point, fire point, smoke point, and acid value, were determined according to ASTM methods.

### 2.5. Optimization studies

For the conversion of ASO to its corresponding biodiesel, the Box-Behnken design of the response surface methodology was applied in

**Table 2**  
Physicochemical properties of ASO.

Properties	Unit	Experimental value
Oil yield	%	64
Moisture Content	%	2.85
Free fatty acid	%	2.96
Density	g/cm <sup>3</sup>	0.92
Acid Value	mg KOH/g	5.89
Viscosity	mm <sup>2</sup> /s	20.5
Specific Gravity		0.93
Iodine Value	gI <sub>2</sub> /100 g	40.66
Peroxide Value	Meq/kg	8.63
Saponification Value	mg KOH/g	158.48

**Table 3**  
Oxide compositions of raw and calcined kaolin.

Components	Raw (%)	Calcined (%)
SiO <sub>2</sub>	58.41	59.96
Al <sub>2</sub> O <sub>3</sub>	32.25	33.79
SO <sub>3</sub>	0.01	0.12
Na <sub>2</sub> O	0.47	0.40
K <sub>2</sub> O	0.49	0.49
CaO	0.05	0.06
MgO	0.73	0.70
TiO <sub>2</sub>	1.68	1.67
Fe <sub>2</sub> O <sub>3</sub>	1.42	1.45
MnO	0.01	0.01
LOI	4.53	1.35

**Table 4**  
Textural properties of raw kaolin, metakaolin and KOH-modified metakaolin.

Sample	Surface area (m <sup>2</sup> /g)	Pore volume(cm <sup>3</sup> /g)	Pore size (nm)
Raw kaolin	173.516	0.086	2.126
Metakaolin	636.531	0.3244	2.113
KMM catalyst	706.906	0.4255	2.118

evaluating the impacts of three independent variables (reaction temperature, reaction time and catalyst concentration) on ASO biodiesel yield. A total of 17 runs were performed. Statistical analysis of variance (ANOVA) was carried out using design expert 11.1.2.0 software. The range and levels of the variables investigated (see Table 1) were chosen based on literature survey [20,26–30]. It should also be mentioned that preliminary experiments were performed to determine the extreme

values of the variables.

The relationship between the biodiesel yield and the independent variables was established by fitting experimental data into a second-order model. The general form of the regression response model is in the form given in Eq. (3).

$$Y = b_0 + \sum_{i=1}^k b_i X_i + \sum_{i=1}^k b_{ii} X_i^2 + \sum_{i<j}^k b_{ij} X_i X_j + e \quad (3)$$

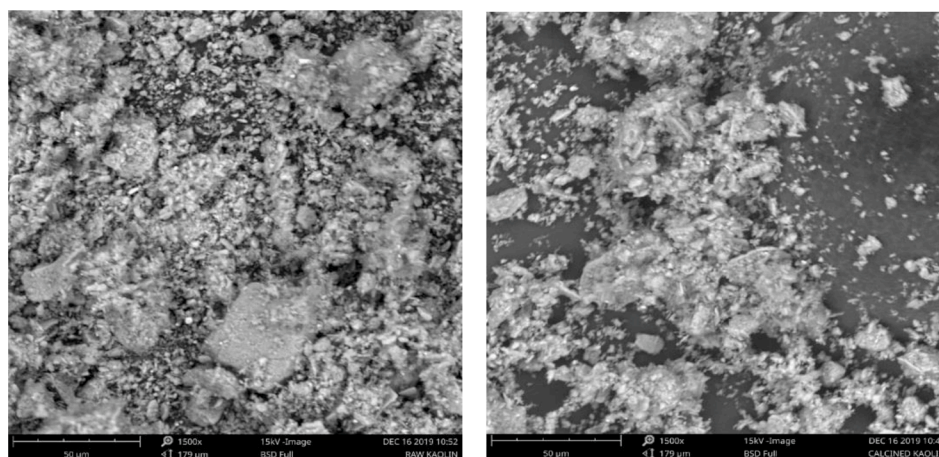
where Y is the response (dependent); X<sub>i</sub> and X<sub>j</sub> are the variables (Independent) variable; b<sub>0</sub> is the intercept; b<sub>i</sub> is the first order coefficient of the model; b<sub>ii</sub> is the quadratic coefficient of i factor; b<sub>ij</sub> is the linear coefficients of the model for the interaction between i and j factors; k is the number of variables optimized in the experiment while e is the error associated with response.

### 3. Results and discussion

#### 3.1. Characterization of extracted ASO

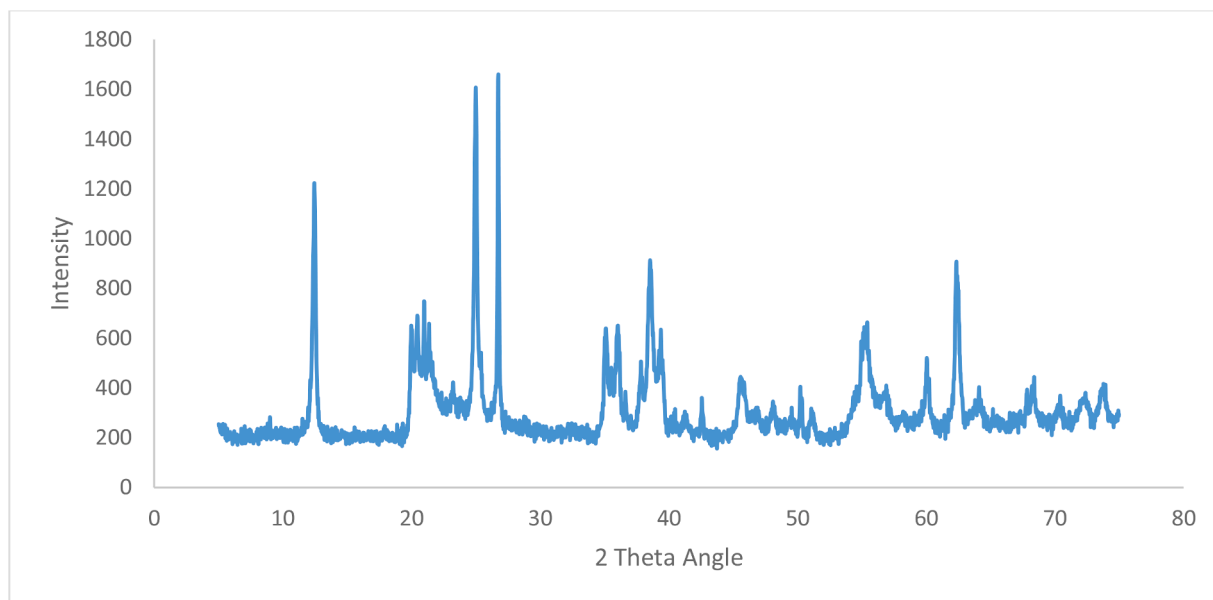
Table 2 presents the physicochemical properties of the Allamanda seed oil. The oil yield from Allamanda seed was 64%, which is higher than the values of 52.79%, 50% and 56.7% reported for oils extracted from *Allandanda cathertica* seed [28], desert date seed [31] and *Jatropha curcas* seed [32], respectively. This appreciably high oil content obtained in this study established the potential of the seed as non-edible oil source for biodiesel production. The low moisture content (2.86%) confirms that the oil is of good quality and was not prone to rancidity easily.

Higher moisture content causes emulsification during transesterification of the oil. The free fatty acid (FFA) value for ASO was 2.75 mg KOH/g with a corresponding acid value of 5.89 mg KOH/g. The acid value for oil required for homogeneous base transesterification should not be greater than 1% (2 mg KOH/g). It is important to state that base activated metakaolin has tolerance for FFA. Hence the oil can be used directly without neutralization. This is an obvious advantage of this catalyst in the transesterification of vegetable oil. The specific gravity of the oil at 25 °C was 0.928 which is a bit higher than the standard value of 0.816. The viscosity of ASO was found to be 20.5 mm<sup>2</sup>/s, hence the need to reduce viscosity through transesterification. Iodine value is used to measure the level of unsaturation in fatty acids in the oil. The limitation of unsaturation of fatty acids is important since heating highly unsaturated fatty acids result in the polymerization of glycerides which can lead to the formation of deposits [5]. The Iodine values of 40.7 gI<sub>2</sub>/100 g

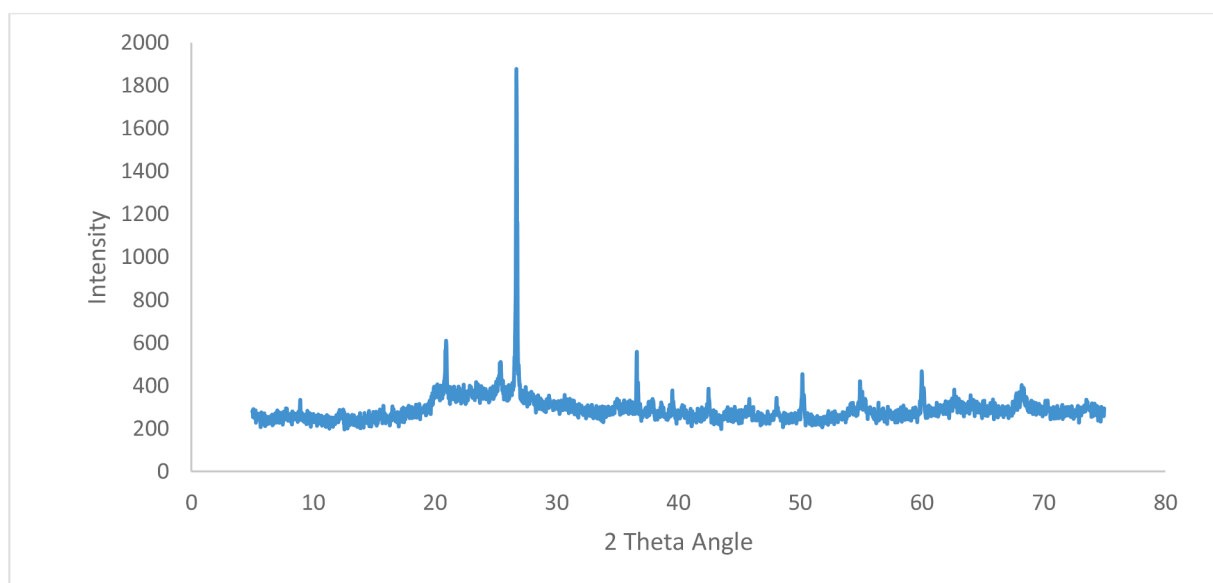


(a) (b)

**Fig. 1.** SEM images of (a) metakaolin and (b) KMM.



(a)



(b)

Fig. 2. XRD patterns of (a) raw kaolin (b) metakaolin (calcined kaolin).

suggest that it is non-drying [33].

### 3.2. Catalyst characterization

The results of oxides composition analysis conducted on the raw and calcined kaolin (see Table 3) revealed that the most abundant oxides in both samples are  $\text{SiO}_2$ ,  $\text{Al}_2\text{O}_3$ ,  $\text{TiO}_2$ , and  $\text{Fe}_2\text{O}_3$ , while  $\text{SO}_3$ ,  $\text{K}_2\text{O}$ ,  $\text{Na}_2\text{O}$ ,  $\text{CaO}$ ,  $\text{MgO}$ , and  $\text{MnO}$  are present in small amount. The  $\text{SiO}_2$  and  $\text{Al}_2\text{O}_3$  compositions increased with about 2% from 58.41 to 59.96% and 32.25% to 33.79% respectively after thermal treatment. The predominance of  $\text{SiO}_2$  and  $\text{Al}_2\text{O}_3$  associated mainly with quarts and kaolinite minerals.  $\text{TiO}_2$  and  $\text{Fe}_2\text{O}_3$  are the main discolouring components and their presence can be associated with hematite, goethite and anatase

materials [34].

Table 4 shows the textural properties of raw kaolin, metakaolin and KOH-modified metakaolin catalyst. It could be seen that raw kaolin had a specific surface area of  $173.52 \text{ m}^2/\text{g}$  which increased to  $636.53 \text{ m}^2/\text{g}$  upon its transformation to metakaolin via calcination process. This observation indicated that the calcination opened up pore on the surface of the calcined kaolin. Also, activation of metakolin with KOH resulted in catalyst with high surface area ( $706.91 \text{ m}^2/\text{g}$ ) as indicated in Table 3, which suggested that the chemical activation had positive influence on the performance of the KMM catalyst due to the increasing BET surface area [35]. The results also indicated that the pore volume and pore size of the KMM catalyst were  $0.4255 \text{ cm}^3/\text{g}$  and  $2.118 \text{ nm}$ , respectively, indicating that the active sites are present on the external surface of the

**Table 5**  
Box Behnken Design matrix for biodiesel yield.

Run	Transesterification process variables			Biodiesel yield		% error
	A: Time (min)	B: Temperature (°C)	C: Catalyst concentration (wt.%)	Experimental value (%)	Predicted value (%)	
1	60	65.0	2.75	78.67	77.04	1.63
2	120	65.0	5.00	82.67	81.05	1.62
3	120	52.5	2.75	76.67	72.47	4.20
4	180	40.0	2.75	75.33	76.96	-1.63
5	120	65.0	0.50	78.67	78.46	0.21
6	60	52.5	5.00	82.00	85.25	-3.25
7	180	52.5	0.50	90.67	87.42	3.25
8	120	40.0	5.00	76.00	76.21	-0.21
9	120	40.0	0.50	62.67	64.29	-1.62
10	120	52.5	2.75	75.67	72.47	3.20
11	120	52.5	2.75	71.67	72.47	-0.79
12	180	52.5	5.00	85.67	83.83	1.84
13	180	65.0	2.75	78.00	81.46	-3.46
14	120	52.5	2.75	67.00	72.47	-5.47
15	120	52.5	2.75	71.33	72.47	-1.14
16	60	52.5	0.50	65.33	67.17	-1.84
17	60	40.0	2.75	66.00	62.54	3.46

**Table 6**  
Regression model fitting and statistical analysis.

Source	Sum of Squares	Df	Mean Square	F Value	p-value Prob>F	
Model	795.46	9	88.38	5.07	0.0219	significant
A-Time	177.35	1	177.35	10.17	0.0153	
B-Temperature	180.50	1	180.50	10.35	0.0147	
C-Catalyst Concentration	105.12	1	105.12	6.03	0.0438	
AB	25.00	1	25.00	1.43	0.2702	
AC	117.36	1	117.36	6.73	0.0357	
BC	21.78	1	21.78	1.25	0.3007	
A <sup>2</sup>	66.53	1	66.53	3.81	0.0918	
B <sup>2</sup>	15.87	1	15.87	0.9100	0.3719	
C <sup>2</sup>	84.32	1	84.32	4.83	0.0639	
Residual	122.11	7	17.44			Not significant
Lack of fit	62.42	3	20.81		0.3666	
			14.92	1.39		
Pure Error	59.69	4				
Cor Total	917.571	16				

catalyst, and it can improve diffusion problems due to larger pore size, thus aiding better flow channel [36]. Furthermore, the values of pore size greater 2.0 nm for all the analyzed samples indicated that they are mesoporous materials.

The SEM images of metakaolin and KOH-modified metakaolin are shown in Fig. 1. As seen in Fig. 1a, the metakaolin showed different layers of different sizes, indicating the order of silica and alumina layers in kaolinite [37]. However, alkaline treated metakaolin exhibited a uniform morphology, though with slight disorder as indicated in Fig. 1b.

The XRD patterns of raw kaolin and metakaolin (calcined kaolin) are shown in Fig. 2. As seen from Fig. 2a, the metakaolin exhibited intense peaks showing an ordered structure which are typical of crystalline materials [38]. The peaks of 2 $\theta$  values at 12.5°, 25.0°, 38.5°, 55.2°, and 62.0° represent the crystalline structure of kaolinite with quartz as major impurities having their main peaks at 20.94, 26.69, 36.59, and 50.20°. This observation is consistent with the one reported by Teku [37]. The XRD characteristics peaks of raw kaolin almost disappeared after thermal treatment leading to the formation of metakaolin. Explicitly, disordered metakaolin was formed in this work after dehydroxylation of kaolin at 650 °C for 90 min which could be observed on the XRD pattern of calcined kaolin as the crystalline peaks disappeared and transformed the crystalline kaolin to amorphous metakaolin. This is evident in the drastic drop in the peak intensity in Fig. 2b. The remaining peaks in this range could be ascribed to traces of mica and quartz in calcined kaolin [19].

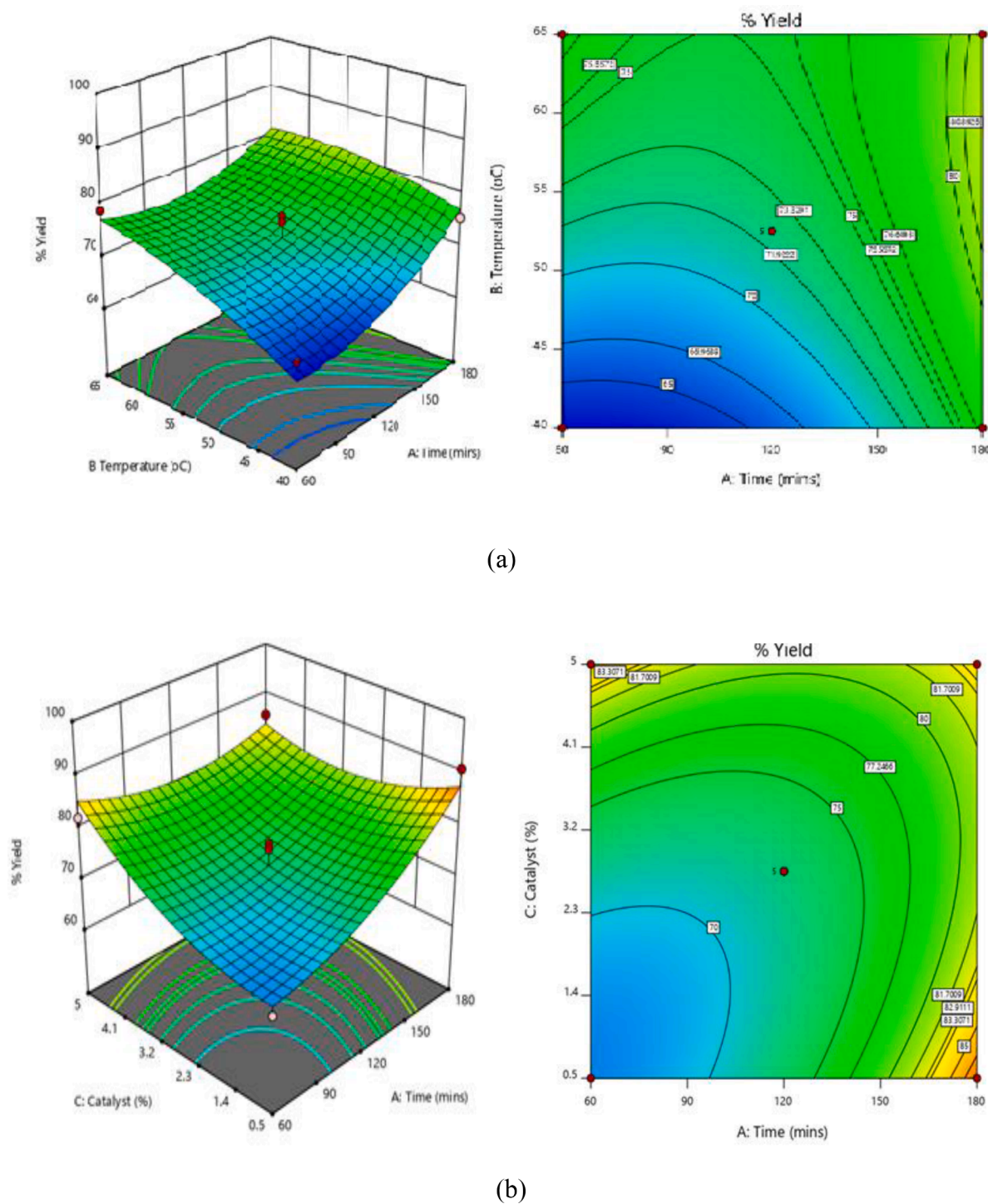
### 3.3. Optimization of biodiesel production process

The BBD matrix as generated by the design expert software and the experimental results obtained in the transesterification of ASO with methanol over KMM catalyst at different conditions are presented in Table 5. A second-order polynomial model that illustrates the relationship between the process response (biodiesel yield) and the studied variables (time, temperature and catalyst loading) is given by Eq. (4).

$$\begin{aligned} \% \text{Yield} = & -19.21520 + 0.098812A + 2.31295B + 5.91975C - 0.003333AB \\ & - 0.040123AC - 0.082963BC + 0.001104A^2 - 0.012427B^2 \\ & + 0.883951C^2 \end{aligned} \quad (4)$$

Positive sign in front of the terms suggests synergistic effect, whereas negative sign implies antagonistic effect. The adequacy of the regression model was evaluated by the coefficient of determination ( $R^2$ ) and standard deviation. The coefficient of determination ( $R^2$ ) measures the degree of fitness of the regression model. According to Akintunde *et al* (2015), a higher  $R^2$  value greater or equal to one depicts a good model fit. The  $R^2$  value of 0.9123 implies that 91.23% of the variability in the response is explained by the model. The value suggests that the regression model equation satisfactorily describes the relationship between the biodiesel yield and variables investigated in this study. The standard deviation of 4.18 shows that the degree of deviation from the response average value is low.

The quality of the model was further justified through analysis of variance (ANOVA). The ANOVA for the quadratic model for biodiesel



(a)

(b)

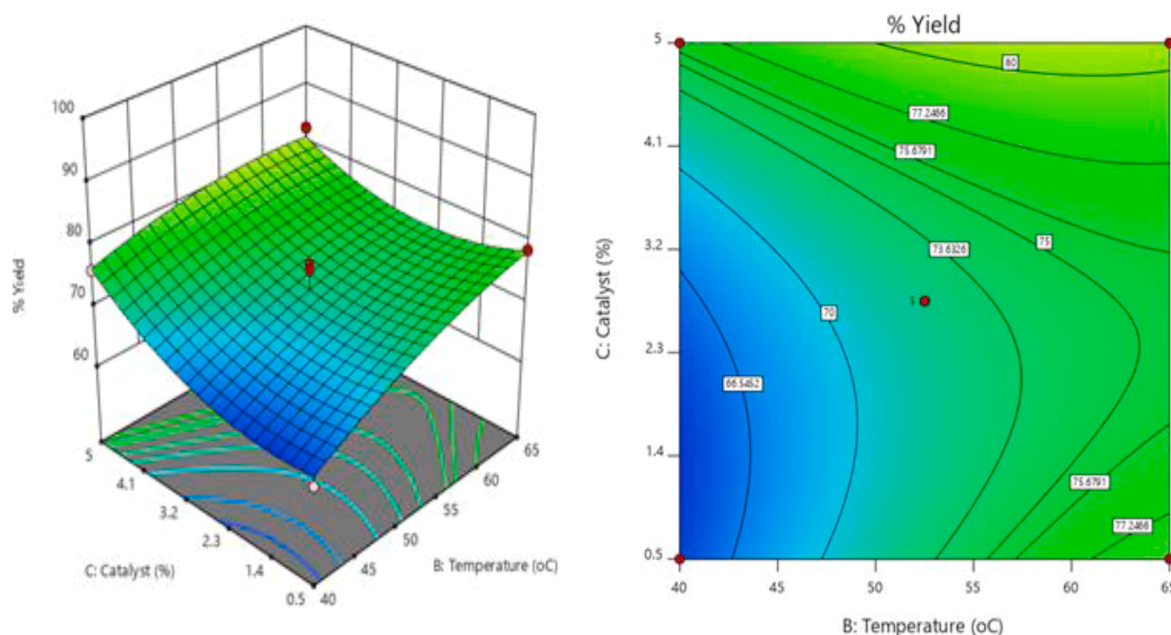
**Fig. 3.** The response surface and contour plots of biodiesel yield as the function of (a) reaction temperature  $T$  ( $^{\circ}\text{C}$ ) and reaction time (min); (b) catalyst concentration (wt.%) and reaction time (min) and (c) catalyst concentration (wt.%) and reaction temperature ( $^{\circ}\text{C}$ ).

yield is presented in Table 6. As contained in the Table, The Model F-value of 5.07 reveals that the model is significant. Values of p-value less than the 0.05 indicates that the model is significant. Herein, A, B, C and AC were significant model terms whereas AB, BC,  $A^2$ ,  $B^2$  and  $C^2$  were not significant to the biodiesel yield. Non-significant lack of fit is good as it confirms the adequacy of the model fit. The result of lack of fit evaluation revealed a p-value of 0.37 which is insignificant. This implies that the regression model developed correlated well with experimental data. Noordin et al. [39] reported that an insignificant lack of fit is highly

desirable since it is a clear indication that nearly all contributions to the response are considered by the regression model.

### 3.3.1. Effect of process variables as response surface plot

The surface plot in Fig. 3(a-c) depicts the interaction effect of the transesterification process variables (reaction temperature, reaction time and catalyst concentration) on ASO biodiesel yield. Fig. 3a illustrates the combined effect of temperature and time on biodiesel yield at constant methanol to oil molar ratio of 5:1 and catalyst loading of 2.75



(c)

Fig. 3. (continued).

Table 7

Fuel properties of ASO biodiesel in comparison with standard.

Properties	Diesel	ASTM D6571	EN	This study
Specific gravity	0.82-0.86	0.88	0.860	0.88
Flash point (°C)	> 55	93 min	130min	152
Cloud point (°C)	-15 to -5	-3-10	-	1.40
Pour point (°C)	-33 to -15	12 max	-15-10	-6.8
Kinematic viscosity (mm <sup>2</sup> /s)	2.5 - 3.5	1.9-6.0	3.5-5.0	4.04
Acid value (mg /KOH)	-0.35	≤0.5	0.5	0.58
Density (g/cm <sup>3</sup> )	0.88	0.86	0.86-0.90	0.88

wt%. The result shows that biodiesel yield increased with increasing reaction temperature and reaction time. The reason for this observation is that high temperature facilitates the diffusion of reactant and dispersion of catalyst particles [40]. Moreover, transesterification reaction reaches equilibrium at high reaction time [41]. The interaction effect of the variables revealed that continuous simultaneous increase in temperature and time improves the biodiesel yield. Fig. 3b shows response surface and contour plots of biodiesel yield as a function of catalyst concentration and reaction time. A rapid improvement in biodiesel yield with increasing catalyst concentration and reaction time has been observed. The presumed reason is that when the amount of catalyst was increased, the amount of available catalytic active sites was enhanced [22]. This is also corroborated by the combined effect of catalyst concentration and reaction temperature (see Fig. 3c), indicating that three variables studied are significant to process response.

### 3.4. Optimal conditions of transesterification of ASO over KMM catalyst

The optimum values for the transesterification process variables studied were numerically predicted to be 180 min, 0.5 wt.% and 52.5 °C for reaction time, catalyst concentration and reaction temperature,

respectively, with 89.65% for ASO biodiesel yield. The prediction was validated by using the best conditions in three replicates, resulting in an average ASO biodiesel yield of  $90.67 \pm 0.14\%$ . Thus, the model accurately represented the transesterification process for biodiesel production from Allamanda seed oil. It is worthy of note that the optimum reaction time and reaction temperature that resulted in maximum biodiesel yield were high and low, respectively. This is because either high temperature or time is required to push reversible transesterification reaction to equilibrium, thereby increasing the biodiesel yield [12].

### 3.5. Characterization of ASO biodiesel

The fuel properties of ASO biodiesel are presented in Table 7 in comparison to fossil diesel and ASTM D6751 and EN 14214 biodiesel specifications.

The kinematic viscosity of Allamanda biodiesel was determined to be 1.04 mm<sup>2</sup>/s as against 20.5 mm<sup>2</sup>/s for raw Allamanda oil. The obvious reduction in viscosity was due to the efficiency of the completion of transesterification. The obtained value falls within the ranges specified by ASTM D6741 and EN 14214 standards for biodiesel. Acid values indicate the age and quality of the biodiesel. The acid value obtained in this work was 0.58 mg KOH/g. The flash point is the minimum temperature required for fuel to ignite when an ignition source is brought close to it. A fuel with a low flash point implies that the fuel is not safe for handling. The flash point obtained in this work is 152 °C, suggesting that the produced ASO biodiesel is safe to be stored and transported [12]. Cloud point is the temperature at which the smallest crystals become noticeable when cooled [42]. The cloud point obtained in this study was 1.40 °C, indicating that the biodiesel produced from ASO has a low tendency for gel formation and therefore can perform satisfactorily under cold climates. The pour point obtained in this work is -6.8 °C, which is within the ASTM D6751 and EN 14214 standard requirements [43].

#### 4. Conclusions

The biodiesel synthesis from Allamanda seed oil via transesterification process using modified metakaolin catalyst was optimized. Effect of operational parameters on the biodiesel yield was evaluated by the Box-Behnken design of response surface methodology. The optimum values of the reaction temperature, reaction time and catalyst concentration were 52.5°C, 180 min and 0.5 wt%, respectively. Analysis of variance revealed a high coefficient of determination ( $R^2 = 0.9123$  and  $Adj - R^2 = 0.8896$ ), thus ensuring a satisfactory adjustment of the second-order regression model with experimental data. The properties of the biodiesel produced under optimum conditions conformed to ASTM D6751 and EN 14214 specifications and as such can be used as a possible alternative to petrodiesel. This study has shown that the application of kaolin derived metakaolin, as well as allamanda seed oil, can be utilised as a potential precursor for eco-friendly and economic production of biodiesel in Nigeria.

#### Declaration of Competing Interest

The authors declare that they have no known competing financial interests or personal relationships that could have appeared to influence the work reported in this paper

#### Data availability

The authors do not have permission to share data.

#### Acknowledgments

The authors acknowledge the Tertiary Education Fund (TETFUND) of Nigeria for providing the grant that financed this research.

#### References

- Hassani, M., Najafpour, G. D., Mohammadi, M., & Rabiee, M. (2014). Preparation, characterization and application of zeolite-based catalyst for production of biodiesel from waste cooking oil.
- Karthikeyan S, Elango A, Prathima A. An environmental effect of GSO methyl ester with ZnO additive fuelled marine engine. *Ind J Geo-Marine Sci* 2014;43(4):564–70.
- Wang E, Ma X, Tang S, Yan R, Wang Y, Riley WW, Reaney MJ. Synthesis and oxidative stability of trimethylolpropane fatty acid triester as a biolubricant base oil from waste cooking oil. *Biomass Bioenergy* 2014;66:371–8.
- Abdullah SHYS, Hanapi NHM, Azid A, Umar R, Juahir H, Khatoon H, Endut A. A review of biomass-derived heterogeneous catalyst for sustainable biodiesel production. *Renewable Sustainable Energy Rev* 2017;70:1040–51.
- Musa U, Aberuagba F. Characteristics of a typical Nigerian *Jatropha curcas* oil seeds for biodiesel production. *Res J Chem Sci* 2012;2(10):7–12.
- Balasubramanian R, Sircar A, Sivakumar P, Ashokkumar V. Conversion of bio-solids (scum) from tannery effluent treatment plant into biodiesel. *Energy Sources, Part A Recovery, Utiliz Environ Effects* 2018;40:959–67.
- Enweremadu CC, Alamu OJ. Development and characterization of biodiesel from shea nut butter. *Int Agrophys* 2010;24(1):29–34.
- Vishnupriya M, Ramesh K, Sivakumar P, Balasubramanian R, Sircar A. Kinetic and thermodynamic studies on the extraction of bio oil from *Chlorella vulgaris* and the subsequent biodiesel production. *Chem Eng Commun* 2019;206:409–18.
- Arunprasad AS, Periyasamy S, Sivakumar P, Sakthisaravanan A, Sircar A. Optimization and kinetic studies on biodiesel production from microalgae (*Euglena sanguinea*) using calcium methoxide as catalyst. *Energy Sources, Part A Recovery, Utiliz Environ Effects* 2019;41:1497–507.
- Lawan I, Garba ZN, Zhou W, Zhang M, Yuan Z. Synergies between the microwave reactor and CaO/zeolite catalyst in waste lard biodiesel production. *Renewable Energy* 2020;145:2550–60.
- Sivagurulingam APA, Sivanandi P, Pandian S. Isolation, mass cultivation, and biodiesel production potential of marine microalgae identified from Bay of Bengal. *Environ Sci Pollut Res* 2022;29:6646–55.
- Yusuff AS, Popoola LT, Adeniyi OD, Olutoye MA. Coal fly ash supported ZnO catalyzed transesterification of *Jatropha curcas* oil: optimization by response surface methodology. *Energy Conv Manag X* 2022. <https://doi.org/10.1016/j.ecmx.2022.100302>.
- Ashokkumar V, Salim MR, Salam Z, Sivakumar P, Chong CT, Elumalai S. Production of liquid biofuels (biodiesel and bioethanol) from brown marine macroalgae *Padina tetrastrum*. *Energy Convers Manag* 2017:135.
- Egwim EC, Ibrahim ZA, Onwuchekwa P. Production and characterization of biodiesel from allamanda cathartica oil. *J Technol Innov Renew Energy* 2013;2(4):388–93.
- Ramirez-Ortiz J, Martinez M, Flores H. Metakaolinite as a catalyst for biodiesel production from waste cooking oil. *Front Chem Sci Eng* 2012;6(4):403–9.
- Sharma YC, Singh B, Korstad J. Advancements in solid acid catalysts for the ecofriendly and economically viable synthesis of biodiesel. *Biofuels, Bioprod Biorefin* 2011;5(1):69–92.
- Sivakumar P, Sivakumar P, Anbarasu K, Mathiarasi R, Renganathan S. An eco-friendly catalyst derived from waste shell of *Scylla tranquebarica* for biodiesel production. *Int J Green Energy* 2014;11:886–97.
- Widayat W, Okvitarini N, Philia J. The effect of impregnated type at kaolin catalyst on biodiesel production from used cooking oil. *AIP Conf Proc* 2020;2197(1):030009. 1-5. <https://aip.scitation.org/doi/pdf/10.1063/1.5140901>.
- Dang, T. H, Chen, B. H., & Lee, D. J (2013). Application of kaolin-based catalysts in biodiesel production via transesterification of vegetable oils in excess methanol.
- Liu J, Yun Z, Gui X. Ce/kaolin clay as an active catalyst for fatty acid methyl esters production from cottonseed oil in a new integrated apparatus. *Braz J Chem Eng* 2018;35:147–54.
- Júnior ODSL, Cavalcanti RM, de Matos TM, Angélica RS, da Rocha Filho GN, Barros IDCL. Esterification of oleic acid using 12-tungstophosphoric supported in flint kaolin of the Amazonia. *Fuel* 2013;108:604–11.
- Yusuff AS, Bhonsle AK, Bangwal DP, Atray N. Development of a barium-modified zeolite catalyst for biodiesel production from waste frying oil: process optimization by design of experiment. *Renewable Energy* 2021;177:1253–64.
- Manojkumar N, Muthukumaran C, Sharmila G. A comprehensive review on the application of response surface methodology for optimization of biodiesel production using different oil sources. *J King Saud Univ-Eng Sci* 2020;34(3):198–208.
- Mansourpoor M, Shariati A. Optimization of biodiesel production from sunflower oil using response surface methodology. *J Chem Eng Process Technol* 2012;3(5):1–5.
- Senthilkumar C, Krishnaraj C, Sivakumar P, Sircar A. Statistical optimization and kinetic study on biodiesel production from a potential non-edible bio-oil of wild radish. *Chem Eng Commun* 2019;206:909–18.
- Abdulkareem, A. S., Jimoh, A., Afolabi, A. S., Odigure, J. O., & Patience, D. (2013). *Production and characterization of biofuel from non-edible oils: an alternative energy sources to petrol diesel* (pp. 171-196). IntechOpen.
- Ajayi O, Teku V, Mukhtar B. Biodiesel production from waste cooking oil using acid-treated Kankara kaolin as catalyst. *Nigerian J Sci Res* 2017;16(1):95–101.
- Egwim EC, Isege SI, Ochigbo S, Akpan G. Production and characterization of biodiesel from Allamanda (Allamanda cathartica) oil using lipase as catalyst. *Biokemistri* 2015;27(4):153. -153.
- Qin F, Meng M, Chang F, Jeje A, Tang Y. Application of modified CaO as an efficient heterogeneous catalyst for biodiesel production. *Indian J Chem Technol* 2017;24:194–7.
- Khurshid SNA. Biodiesel production by using heterogeneous catalyst. M.Sc Thesis submitted to Division of Chemical Technology Department of Chemical Engineering and Technology Royal Institute of Technology (KTH). 2014. Stockholm, Sweden, <https://www.diva-portal.org/smash/get/diva2:721123/FULLTEXT01.pdf>.
- Chapagain BP, Yehoshua Y, Wiesman Z. Desert date (*Balanites aegyptiaca*) as an arid lands sustainable bioresource for biodiesel. *Bioresour Technol* 2009;100(3):1221–6.
- Yusuff AS. Parametric optimization of solvent extraction of *Jatropha curcas* seed oil using design of experiment and its quality characterization. *S Afr J Chem Eng* 2021;35:60–8.
- Musa U, Isah AG, Mohammed IA, Garba MU, Usman Z, Alhassan B. Extraction of *Chrysophyllum albidum* seed oil: optimization and characterization. *Chem Process Eng Res*, vo 2015;30:1–9.
- Oyebanjo O, Ekosse GI, Odiyo J. Physico-chemical, mineralogical and chemical characterization of cretaceous-paleogene/Neogene kaolins within Eastern Dahomy and Niger Delta Basins from Nigeria: possible industrial applications. *Minerals* 2020;10:670. <https://doi.org/10.3390/min10080670>.
- Ramirez-Ortiz J, Medina-Valtierra J, Rosales MM. Used frying oil for biodiesel production over kaolinite as catalyst. *Eng Technol* 2011;80:977–80.
- Tan TH, Abdullah MO, Nolasco-Hipolito C, Taufiq-Yap YH. Waste ostrich- and chicken-eggshells as heterogeneous base catalyst for biodiesel production from used cooking oil: catalyst characterization and biodiesel yield performance. *Appl Energy* 2015;160:58–70.
- Teku VD. Modified kaolinite clay as catalyst for biodiesel production from waste cooking oil. Zaria. Nigeria: Department of Chemical Engineering, Ahmadu Bello University; 2017.
- Tironi A, Trezza MA, Irassar EF, Scian AN. Thermal treatment of Kaolin: effect on the pozzolanic activity. 11<sup>th</sup> International congress on metallurgy & materials SAM/CONAMET 2011. *Proc Mater* 2012;1:343–50. <https://doi.org/10.1016/j.mspro.2012.06.046>.
- Noordin MY, Venkatesh VC, Sharif S, Elting S, Abdullah A. Application of response surface methodology in describing the performance of coated carbide tools when turning AISI 1045 steel. *J Mater Process Technol* 2004;145(1):46–58.
- Olutoye MA, Hameed BH. A highly active clay-based catalyst for the synthesis of fatty acid methyl ester from waste cooking palm oil. *Appl Catal*, A 2013;450:57–62.
- Olutoye MA, Wong SW, Chin LH, Amani SW, Asif M, Hameed BH. Synthesis of fatty acid methyl esters via the transesterification of waste cooking oil by methanol with

- a barium-modified montmorillonite K10 catalyst. *Renewable Energy* 2016;86:392-8.
- [42] Salaheldeen M, Aroua MK, Mariod AA, Cheng SF, Abdelrahman MA, Atabani AE. Physicochemical characterization and thermal behaviour of biodiesel and biodiesel–diesel blends derived from crude *Moringa peregrina* seed oil. *Energy Convers Manage* 2015;92:535–42.
- [43] Yusuff AS, Gbadamosi OA, Atray N. Development of a zeolite supported CaO derived from chicken eggshell as active base catalyst for used cooking oil biodiesel production. *Renewable Energy* 2022;197:1151–62.